EurJIC
European Journal of Inorganic Chemistry

Research Article
doi.org/10.1002/ejic.202200528

Chemistry Europe
European Chemical Societies Publishing

www.eurjic.org

Isomerism in Hexacoordinate Ti(IV) and Zr(IV) Complexes with a Tetradentate ONNO-*Schiff* Base Ligand

Bahareh Rezaei Kheirkhah[+],[a] Tareq M. A. Al-Shboul[+],[a, b] Felix Edwin Pröhl,[a] Sven Krieck,[a] Helmar Görls,[a] and Matthias Westerhausen*[a]

The reactions of $[(thf)_2TiCl_4]$ with sodiated 2,2′-bis[2-hydroxy-3,5-di(*tert*-butyl)benzylideneamino]-1,1′-biphenyl (**1 a**) and 2,2′-bis[2-hydroxy-3,5-di(*tert*-butyl)benzylideneamino]-4,4′-dimethyl-1,1′-biphenyl (**1 b**) yield the corresponding Ti complexes **2 a** and **2 b**. Similarly, **1 a** reacts with $[(thf)_2ZrCl_4]$ to the corresponding Zr derivative **3**. For **2 a**, a mixture of *cis*-β and *trans* isomers were observed in solution whereas the Zr congener exclusively forms the *cis*-α form. Quantum chemical calculations verify that these isomers are the preferred molecular structures. The crystal structures of *cis*-β isomeric **2 a** and *cis*-α isomeric **3** have been determined. Metalation of **1 a** with $Ti(NMe_2)_4$ yields 2,2′-bis[(2-oxido-3,5-di(tert-butyl)phenyl)-dimethylaminomethylamino]-1,1′-biphenyl titanium(IV) (**4**) with a hexadentate ligand.

Introduction

Ligands with an ONNO binding motif play a crucial role in coordination chemistry due to diverse and broad applications in many fields such as bioinorganic, medicinal, inorganic, organometallic, and macromolecular chemistry as well as catalysis, the most prominent representatives being the salen ligand **I**, prepared from salicylaldehyde (sal) and ethylenediamine (en), as well as derivatives thereof (Scheme 1A).[1] The broad and deep impact of this highly valued ligand class is founded on the easy and straightforward access of these *Schiff* base ligands as well as their stability and inertness in metal complexes. The *Jacobsen* ligand **II** with a cyclohexane-1,2-diyl backbone and the related congener with a (substituted) 1,1′-biphenyl-2,2′-diyl backbone **III** allow the introduction of chirality for catalytic applications of their metal complexes. In octahedral complexes, these ligand systems can adopt *trans*, *cis*-α and *cis*-β binding modes shown in Scheme 1B. The preferred isomeric structure can be influenced by the substitution patterns at the salicyl units and at the backbone substructures. The cyclohexyl fragment of the *Jacobsen* ligand **II** freezes C_2 symmetry with a

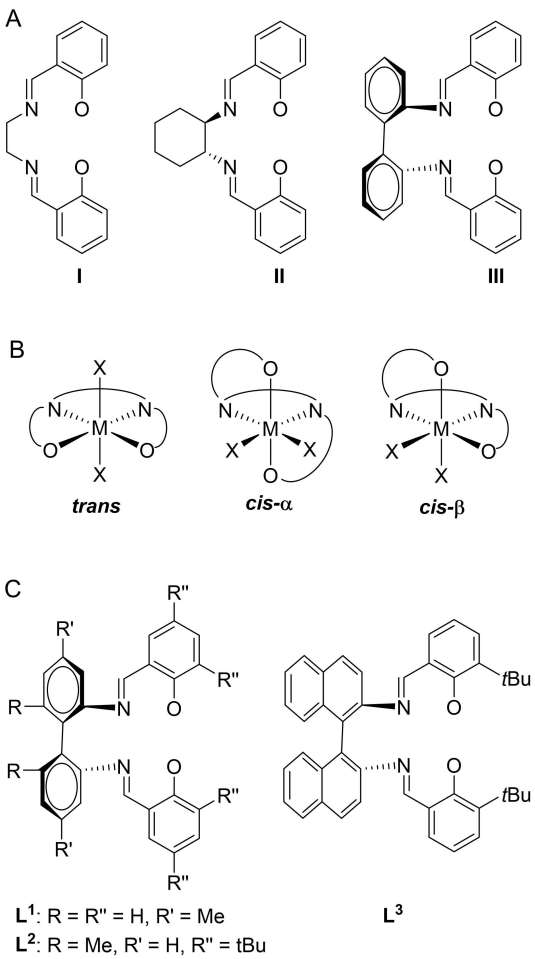

Scheme 1. (A) Prominent ligands derived from the salen ligand (left) with 1,2-cyclohexanediyl (middle) and 1,1′-biphenyl-2,2′-diyl backbones. (B) Isomerism of such tetradentate ligands with an ONNO binding motif. In the *trans* isomer all donor atoms are bonded meridionally, in the *cis*-α isomer the two NNO donor sites exhibit a facial arrangement, in *cis*-β one NNO pocket shows facial, the other meridional coordination modes. (C) ONNO ligands that have been studied earlier in titanium complexes (see text).

[a] *B. Rezaei Kheirkhah,[+] Prof. T. M. A. Al-Shboul,[+] Dr. F. E. Pröhl, Dr. S. Krieck, Dr. H. Görls, Prof. M. Westerhausen*
Institute of Inorganic and Analytical Chemistry
Friedrich Schiller University Jena (FSU)
Humboldstraße 8, 07743 Jena, Germany
E-mail: m.we@uni-jena.de
www.westerhausen.uni-jena.de
[b] *Prof. T. M. A. Al-Shboul[+]*
Department of Chemistry and Chemical Technology
Tafila Technical University (TTU)
P.O. Box 179, 66110 Tafila, Jordan
[+] *These authors contributed equally.*

Supporting information for this article is available on the WWW under https://doi.org/10.1002/ejic.202200528

Research Article
doi.org/10.1002/ejic.202200528

rather rigid binding pocket. Contrary to this coordination behavior, ligand **III** with the biphenyl moiety is quite flexible due to rotational freedom around the C–C bond of the aryl units of the biphenyl substructure.

In complexes of the hexacoordinate Group IV metals with (substituted) tetradentate 2,2′-bis(2-oxidobenzylideneamino)-1,1′-biphenyl ligands all isomers had already been observed. Unstrained red 2,2′-bis(2-oxidobenzylideneamino)-4,4′-dimethyl-1,1′-biphenyl titanium(IV) dichloride (L^1)$TiCl_2$ crystallized as *trans* isomer whereas in solution an equilibrium between *trans* and *cis-β* forms existed.[2] The *trans* isomer was also preferred for unstrained [(salen)TiX_2] (X=F,[3] Cl,[4] Me,[5] OC_6H_4-4-*t*Bu[6]) complexes. Bulky *tert*-butyl groups at the salicyl substituents in (L^2)$TiBr_2$ stabilized the *cis-α* isomer whereas in solution, both *cis* isomers were present.[7] Exchange of the halide ions by alkoxides in (L^3)Ti(O*i*Pr)$_2$ also led to crystallization of the *cis-α* isomeric molecule.[8] Generally, zirconium(IV) complexes crystallized as *cis-α* isomers[9–11] as had been observed for the hafnium(IV) congener, too.[10]

This brief overview on structural behavior of Group IV complexes with 2,2′-bis(2-oxidobenzylideneamino)-1,1′-biphenyl-derived ONNO-*Schiff* base ligands encouraged us to study the isomerization processes of such [(L)$TiCl_2$] compounds. In principle, two pathways seemed to be possible. The dissociative mechanism would yield an ion pair of the type [(L)TiCl]$^+$ Cl^- allowing a subsequent reorientation of the coordination sphere at the pentacoordinate titanium center, mechanistically comparable to the *Berry* pseudo-rotation. The fact that isomerization also occurred in hydrocarbon solvents disfavored this proposal and reinforced an intramolecular isomerization process similarly to the *Bailar* and *Rây-Dutt* twist mechanisms that had been observed for octahedral complexes with bidentate ligands. The intermediate transition state would adopt a trigonal prismatic structure. However, depending on the rotation axis of opposite triangular faces several isomeric forms seemed feasible. These intermediate prismatic structures are depicted in Scheme 2.

We did not introduce any steric pressure at the biphenyl backbone (R=H, see Scheme 1C) but used 3,5-di(*tert*-butyl)salicyl sidearms in this ligand (R″ = *t*Bu) to disfavor the planar arrangement of the ONNO *Lewis* donor sites and, hence, formation of the *trans* complex. This preparative investigation was supported by quantum chemical studies to identify the thermodynamically preferred molecular structure and probable isomerization pathways.

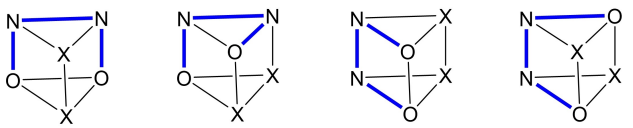

Scheme 2. Isomeric trigonal prismatic forms generated by rotation of opposite triangular faces of the octahedral complex with a tetradentate ONNO ligand system shown in blue. The Ti atom which would be located in the center of the trigonal prism is neglected for clarity reasons.

Results and Discussion

Preparative Investigations

The synthesis of the *Schiff* bases 2,2′-bis[2-hydroxy-3,5-di(*tert*-butyl)benzylideneamino]-1,1′-biphenyl (**1 a**; R = R′ = H, R″ = *t*Bu in Scheme 1C) and 2,2′-bis[2-hydroxy-3,5-di(*tert*-butyl)benzylideneamino]-4,4′-dimethyl-1,1′-biphenyl (**1 b**; R = H, R′ = Me, R″ = *t*Bu) succeeded with good yields via condensation of the corresponding 2,2′-diamino-1,1′-biphenyl with 3,5-di(*tert*-butyl)salicylaldehyde in ethanol. Deprotonation of the hydroxy functionalities in THF with sodium hydride and subsequent metathetical reactions with [$(thf)_2TiCl_4$] and [$(thf)_2ZrCl_4$] yielded the corresponding Group IV complexes of Ti (**2 a** and **2 b**) and Zr (**3**) as depicted in Scheme 3. These compounds were recrystallized from various solvents and solvent mixtures such as diethyl ether/pentane or toluene/hexane for red **2 a**, acetonitrile for red **2 b** and THF/pentane for yellow **3**. The NMR solutions in [D_6]benzene showed two isomers for **2 a** (*cis-β* as well as *cis-α* or *trans* forms, Figure S5) but only the *cis-α* isomer for the Zr derivative **3** (Figure S11) The *cis-α* or *trans* isomers have two chemically equivalent salicyl subunits and cannot be distinguished by NMR spectroscopy. The chemical shifts and shape of the ^{1}H NMR signals of **2 a** show a strong temperature dependency hinting toward isomerization processes in solution (Fig-

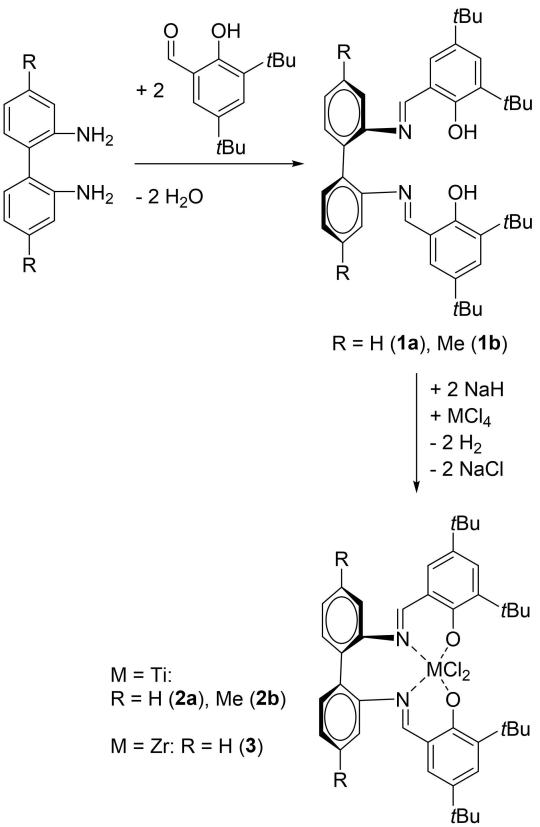

Scheme 3. Syntheses of the *Schiff* base ligands 2,2′-bis[2-hydroxy-3,5-di(*tert*-butyl)benzylideneamino]-1,1′-biphenyl (**1 a**) and 2,2′-bis[2-hydroxy-3,5-di(*tert*-butyl)benzylideneamino]-4,4′-dimethyl-1,1′-biphenyl (**1 b**) and their titanium(IV) and zirconium(IV) complexes.

Research Article
doi.org/10.1002/ejic.202200528

ure S6). This interpretation was verified by cross peaks in the EXSY NMR experiments (Figure S8).

Structural Studies

In the compounds **1a** and **1b**, weak intramolecular O–H···N hydrogen bridges stabilize the planar 2-hydroxybenzylideneamino unit, and no short intermolecular contacts disturb this arrangement. Despite small changes (additional methyl groups in 4,4′-positions of the biphenyl backbone) the molecular structures are quite different in the crystalline phase due to rotation around the C–C bond of the biphenyl substructure. Molecular structure and atom labeling scheme of compound **1b** are depicted in Figure 1, derivative **1a** is shown in the ESI (Figure S15).

Selected structural parameters of **1a** and **1b** are listed in Table 1. The parameters are very similar and independent from the packing and conformation of the molecules in the crystalline state. All bond lengths lie in the expected range and the methyl groups at the biphenyl backbone expectedly have no influence on the structural parameters.

Molecular structure and atom labeling scheme of the Ti complex **2a** are depicted in Figure 2, congener **2b** is depicted in the ESI (Figure S16). Both compounds crystallize as *cis*-β isomers. Deprotonation and coordination alter the structural parameters of the ligand system insignificantly (Table 1) but the C7–N1–C8 bond angle becomes narrower upon coordination to the titanium atom. The larger coordination number of 3 for N1 due to the additional Ti1–N1 bond does not elongate the N1–C7 and N1–C8 bonds. The chloride ligands are in different chemical environments, one anion is *trans* to an oxygen atom, the other *trans* to a nitrogen atom. The latter shows smaller Ti–Cl distances. The Ti–N bonds *trans* arranged to an oxygen base are significantly shorter than the other one *trans* positioned to the chloride ligand.

The zirconium(IV) complex **3** crystallizes as *cis*-α isomer. The molecular structure and atom labeling scheme are depicted in Figure 3. Both chloride ligands are trans positioned to nitrogen bases and this higher symmetry leads to very similar Zr1–Cl1 and Zr1–Cl2 distances. The larger radius of Zr and hence larger bond lengths lead to narrower angles to the tetradentate ONNO ligand because the bite of the ligand binding pockets are rather rigid. In addition, the C7–N1–C8 and C19–N2–C20 bond angles with values of 114.06(18)° and 114.19(19)°, respectively, are narrower than observed in the titanium complexes.

Substitution of the chloride ions in **2a** by dimethylamido ligands led to destabilization of the complex and degradation was observed by NMR spectroscopy yielding several unknown species. Therefore, compound **1a** was deprotonated with $Ti(NMe_2)_4$ in pentane solution. The yellow solution turned red immediately. Reduction of the volume of the solution in vacuo

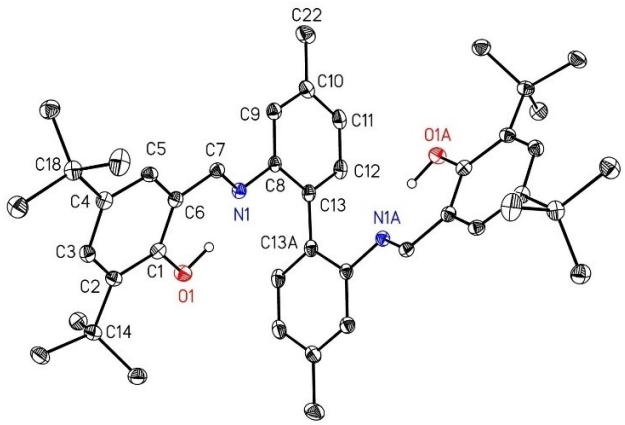

Figure 1. Molecular structure and atom labelling scheme of compound **1b**. Symmetry-related atoms (−x+1, −y+1, z) are marked with the letter "A". The ellipsoids represent a probability of 30%, C-bound hydrogen atoms are omitted for the sake of clarity. Selected structural parameters are listed in Table 1.

Table 1. Selected structural parameters (bond lengths [pm] and angles [deg.]) of compounds **1a** and **1b**.

Comp.	1a	1b	2a	2b
O1–C1	135.6(3)	135.3(2)	134.6(4)	134.4(5)
O1–$H1_{O1}$	98(3)	98(3)	–	–
N1–C7	128.9(3)	128.7(3)	128.5(4)	127.8(6)
N1–C8	141.0(3)	141.7(3)	144.4(4)	145.4(6)
C1–C2	140.2(3)	140.4(3)	140.8(4)	139.4(6)
C1–C6	141.6(3)	141.3(3)	140.5(5)	141.8(6)
C2–C3	139.6(3)	139.2(3)	138.7(5)	140.6(6)
C3–C4	140.0(3)	140.3(3)	140.9(5)	141.0(6)
C4–C5	138.3(3)	138.2(3)	137.3(4)	136.5(6)
C5–C6	139.7(3)	140.1(3)	140.4(5)	140.8(6)
C6–C7	144.4(3)	145.2(3)	144.3(4)	144.8(6)
C13–C13 A	149.4(5)	149.0(4)	149.2(5)	147.8(7)
C7–N1–C8	120.7(2)	122.67(18)	115.1(3)	116.2(4)

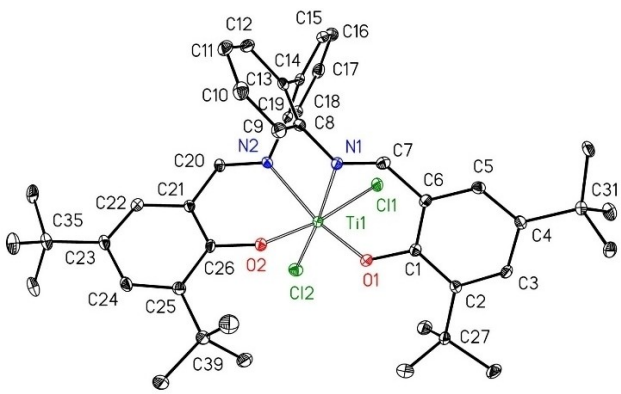

Figure 2. Molecular structure and atom labelling scheme of the *cis*-β isomer of compound **2a**. The ellipsoids represent a probability of 30%, hydrogen atoms are neglected for the sake of clarity. Selected bond lengths (pm): Ti1–O1 183.6(2), Ti1–O2 184.6(2), Ti1–N1 222.2(3), Ti1–N2 218.1(3), Ti1–Cl1 231.42(10), Ti1–Cl2 230.44(10); angles (deg.): O1–Ti1–O2 97.63(10), O1–Ti1–N1 82.47(10), O1–Ti1–N2 163.11(10), O1–Ti1–Cl1 91.29(8), O1–Ti1–Cl2 103.83(8), O2–Ti1–N1 91.54(10), O2–Ti1–N2 82.29(10), O2–Ti1–Cl1 170.72(7), O2–Ti1–Cl2 89.57(8), N1–Ti1–N2 80.65(10), N1–Ti1–Cl1 87.10(7), N1–Ti1–Cl2 173.41(7), N2–Ti1–Cl1 88.44(7), N2–Ti1–Cl2 93.06(7), Cl1–Ti1–Cl2 90.76(4). Additional structural parameters are listed in Table 1.

Research Article
doi.org/10.1002/ejic.202200528

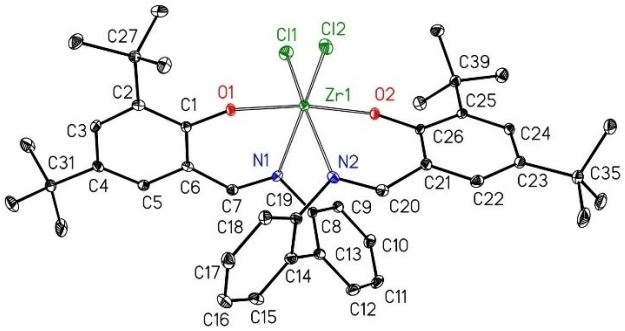

Figure 3. Molecular structure and atom labelling scheme of the *cis-α* isomer of compound **3**. The ellipsoids represent a probability of 30 %, hydrogen atoms are neglected for the sake of clarity. Selected bond lengths (pm): Zr1–O1 199.32(16), Zr1–O2 200.19(16), Zr1–N1 232.28(18), Zr1–N2 232.83(19), Zr1–Cl1 241.45(6), Zr1–Cl2 241.53(6); angles (deg.): O1–Zr1–O2 170.50(6), O1–Zr1–N1 77.24(6), O1–Zr1–N2 97.05(6), O1–Zr1–Cl1 92.21(5), O1–Zr1–Cl2 92.62(4), O2–Zr1–N1 93.83(6), O2–Zr1–N2 76.99(6), O2–Zr1–Cl1 91.62(5), O2–Zr1–Cl2 94.75(5), N1–Zr1–N2 73.09(6), N1–Zr1–Cl1 93.86(5), N1–Zr1–Cl2 158.75(5), N2–Zr1–Cl1 161.78(5), N2–Zr1–Cl2 89.99(5), Cl1–Zr1–Cl2 105.27(2).

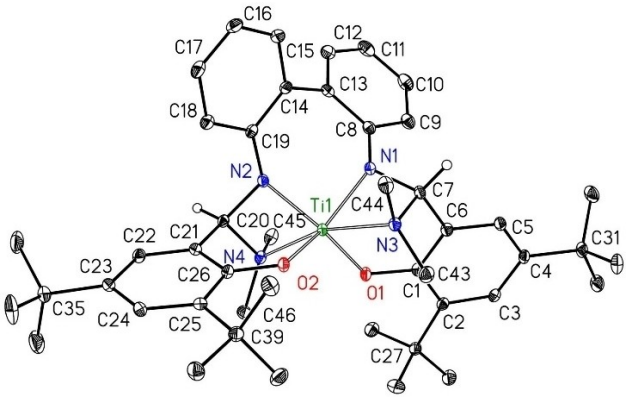

Figure 4. Molecular structure and atom labelling scheme of compound **4**. The ellipsoids represent a probability of 30 %, hydrogen atoms are neglected for the sake of clarity except those at C7 and C20. Selected bond lengths (pm): Ti1–O1 192.34(18), Ti1–O2 191.70(18), Ti1–N1 195.4(2), Ti1–N2 196.2(2), Ti1–N3 225.2(2), Ti1–N4 222.3(2), O1–C1 135.6(3), O2–C26 135.3(3), C7–N1 145.9(3), C7–N3 151.4(3), C6–C7 151.0(3), C20–N2 146.2(3), C20–N4 150.6(3), C20–C21 150.9(3), N3–C43 147.4(3), N3–C44 148.2(3), N4–C45 148.4(3), N4–C46 147.8(3); angles (deg.): O1–Ti1–O2 116.78(8), O1–Ti1–N1 93.01(8), O1–Ti1–N2 135.63(9), O1–Ti1–N3 87.01(8), O1–Ti1–N4 82.90(8), O2–Ti1–N1 135.90(9), O2–Ti1–N2 91.67(8), O2–Ti1–N3 85.43(8), O2–Ti1–N4 88.62(8), N1–Ti1–N2 87.46(9), N1–Ti1–N3 63.22(8), N1–Ti1–N4 128.91(9), N2–Ti1–N3 131.01(9), N2–Ti1–N4 63.39(8), N3–Ti1–N4 164.49(8).

led to precipitation of crystals. However, these red crystals were covered with an oily residue and isolation of pure material failed. Nevertheless, we were able to determine the crystal structure by X-ray diffraction experiments. Obviously, the Ti–NMe_2 moieties added onto the imine functionalities leading to 2,2′-bis[(2-oxido-3,5-di(tert-butyl)phenyl)-dimethylaminomethylamino]-1,1′-biphenyl titanium(IV) (**4**) with a hexadentate ligand as depicted in Scheme 4. However, this reaction led to two chiral carbon atoms (marked with *) enhancing the number of possible isomers and of the resonances in the NMR spectra. This kind of migratory insertion of a metal-bound group to an imine carbon had been observed earlier for benzyl groups bound at titanium[7] and zirconium.[12]

Molecular structure and atom labeling scheme of **4** are depicted in Figure 4. Due to the centrosymmetric monoclinic space group $P2_1/n$ the crystal contains a racemate. The Ti1 atom is in a distorted octahedral environment with a planar ONNO binding motif of the 2,2′-disalicyliminato-1,1′-biphenyl unit with the dimethylamino substituents coordinating with a *transoid* arrangement. The molecular structure of **4** verifies that a *trans* arrangement as preferred for unstrained salen complexes of titanium(IV) cannot safely be prevented by *tert*-butyl substituents in 3-position of the salicyl moieties.

Addition of two equivalents of $KPPh_2$ to a solution of zirconium complex **3** in heptane and toluene led to immediate color change from yellow to deep dark red. A ^{31}P NMR spectrum of the reaction mixture verified that degradation occurred and no zirconium-bound diphenylphosphanide anions were observed. The phosphorus-containing species were primarily $HPPh_2$ (doublet at $\delta(^{31}P) = -40.7$ ppm) and $Ph_2P\text{-}PPh_2$ (singlet at $\delta(^{31}P) = -14.9$ ppm), and we were unable to isolate a well-defined Zr compound. The formation of diphenylphosphane and tetraphenyldiphosphane hinted toward radical pathways as proposed earlier for the reaction of β-diketiminato zirconium trichloride with $KPPh_2$.[13]

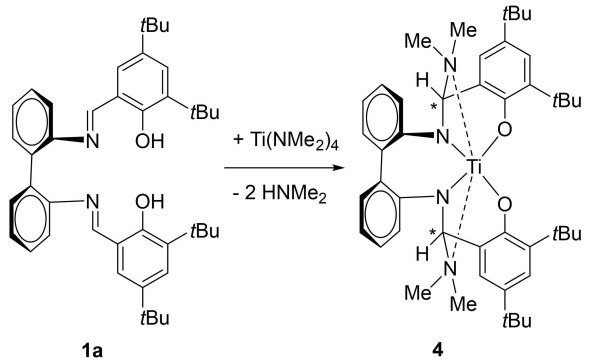

Scheme 4. Synthesis of 2,2′-bis[(2-oxido-3,5-di(tert-butyl)phenyl)-dimethylaminomethylamino]-1,1′-biphenyl titanium(IV) (**4**) via metalation of **1a** with $Ti(NMe_2)_4$.

Computational Investigations

To identify the preferred molecular structures of **2a** and **3** we performed DFT calculations. In addition, these quantum chemical studies should clarify whether the second isomer in solutions of **2a** is the *cis-α* or the *trans* arrangement of the chloride ligands as well as the influence of the metal radius on the preferred isomeric form because the homologous compounds crystallize in different isomeric forms.

Since the SDD/RPW6B95[14–16] level of theory proved to be fast and reliable in a comparative study on Zr,[17] it was chosen for geometry optimization and frequency analysis of both **2a** and **3**.

Research Article
doi.org/10.1002/ejic.202200528

The radius of the metal atom influences the preferred molecular structure, and the *cis-β* isomer is favored for the Ti compound **2a** whereas the *cis-α* form is lowest in energy for the Zr congener **3**. Those compounds were also the experimentally observed isomers and it could be concluded that the second isomer, which is observed in the NMR spectra of solutions of **2a**, was the *trans* isomer. However, the differences between the calculated energies of the isomers are very small and lie below 10 kJ mol^{-1} (Figure 5). Since the optimized structures exhibit many low-lying vibration modes, we neglected thermal corrections (Table S2 lists the respective Gibbs free energies according to pure harmonic oscillator and hindered rotator models).

To account for dispersion effects within the ligand backbone and across the metal center, the M062X[18] functional was employed in conjunction with Grimme's D3 empirical dispersion correction.[19] The solvent effects of toluene, from which the crystals of **2a** were obtained, were considered with the SMD solvation model as implemented in Gaussian16.[20] Both levels of theory confirmed the RPW6B95 ranking and gave similarly small differences for the isomers (see Table S2).

Transformation of one isomer into another was investigated only for the titanium derivative because isomerization processes were observed in NMR experiments, whereas only *cis-α* isomeric zirconium compounds are known and the NMR spectra do not point to isomerization processes. On the contrary, all possible isomers had already been observed for crystalline titanium derivatives depending on substitution patterns and crystallization conditions. The two transition states TS1 and TS2 (see Scheme 5 and Figure 5) were found by manual modelling and subsequent optimization. The dissociation of one chloride ion was investigated as well. The respective energies starting from the *cis-β* isomer, with Cl1 *trans* to a nitrogen leaving via TS3 and Cl2 *trans* to an oxygen leaving via TS4 are shown in Figure 5.

As expected from the crystal structure, TS3 along the dissociation path of chlorine atom Cl1, which is furthest away from the metal center, requires less energy. Note, that the asymmetry within the coordination sphere is most pronounced for the *cis-β* complex. The *cis-α* and *trans* isomers were optimized to almost C_2 symmetric molecules. The dissociation paths starting from the *cis-α* and the *trans* isomers lead to symmetry equivalent transition states (TS4), which are about 50 kJ/mol higher in energy (see Table S3 and Figure S17). A dissociative mechanism for interconversion of different isomers via fivefold coordinated complexes and subsequent pseudorotation can thus be ruled out so that an intramolecular mechanism without metal-ligand bond cleavage is preferred.

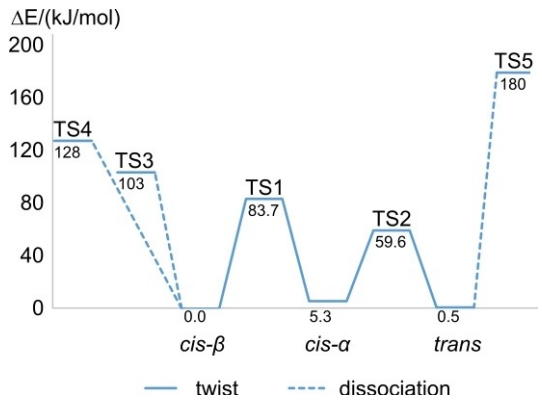

Figure 5. Predicted relative sum of electronic and zero point energy of the isomers of **2a** and transition states of the twist (blue solid lines) and dissociation mechanisms (blue dashed lines). The energy values are given underneath the energy levels (SDD/RPW6B95). A direct conversion of the *cis-β* isomer into the *trans* compound had not been identified.

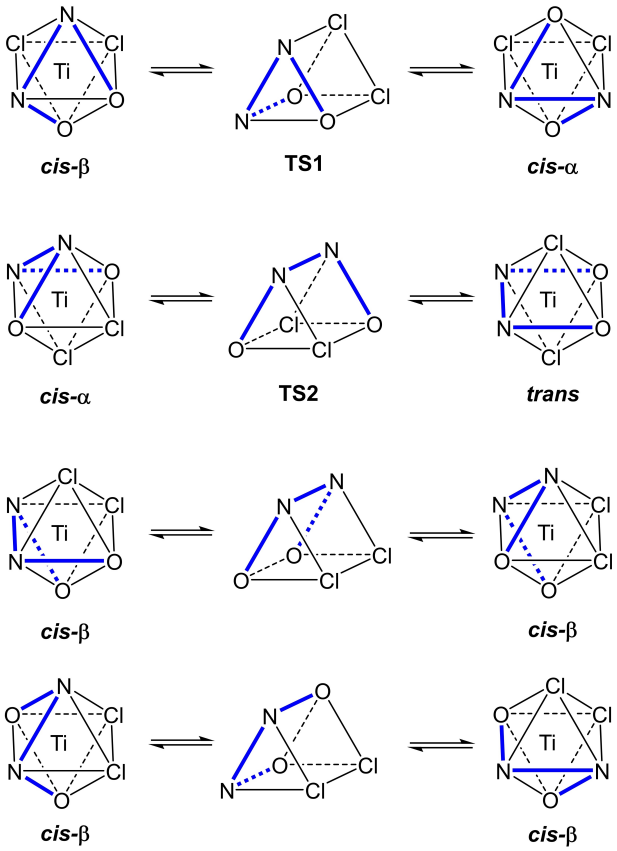

Scheme 5. Isomerization processes via rotation of opposite triangular faces against each other (*Bailar* twist), leading to intermediate trigonal prismatic coordination spheres of the titanium atoms in contrast to a *Rây-Dutt* twist which is based on a rotation around a pseudo C_3 axis (see text).

Conclusions

Metalation of the *Schiff* bases 2,2′-bis[2-hydroxy-3,5-di(*tert*-butyl)benzylideneamino]-1,1′-biphenyl (**1a**) and 2,2′-bis[2-hydroxy-3,5-di(*tert*-butyl)benzylideneamino]-4,4′-dimethyl-1,1′-biphenyl (**1b**) with sodium hydride and subsequent metathetical reaction with $TiCl_4$ yields the respective titanium(IV) complexes **2a** and **2b**. A similar reaction of **1a** with $ZrCl_4$ gives the corresponding zirconium(IV) congener **3**. To probe these compounds as hydroamination catalysts, substitution of the chloride ligands of **2a** by dimethylamido ligands via a metathetical approach fails and various side reactions lead to

Research Article
doi.org/10.1002/ejic.202200528

degradation. An alternative route offers the metalation of **1a** with $Ti(NMe_2)_4$. Deprotonation of **1a** proceeds smoothly, however, immediate addition of the Ti-bound NMe_2 ligands onto the imine functionalities leads to a hexadentate NONNON ligand with *trans*-arranged dimethylamino groups.

In solution, the titanium(IV) complexes show the two isomeric *cis*-β and *trans* forms, whereas for the zirconium(IV) compound **3** only the *cis*-α isomer has been observed in the crystalline state and in solution. Quantum chemical investigations verify that the *cis*-α isomer is favored for the Zr derivative, whereas the energy difference between the *cis*-β and *trans* isomers of the Ti compounds is very small leading to a coexistence of these isomers. Interconversion between these isomers is feasible via rotation of two opposite triangular faces.

Experimental Section

General procedures. All manipulations were carried out under an inert nitrogen atmosphere using standard *Schlenk* techniques. The solvents were dried over KOH and subsequently distilled over sodium/benzophenone under a nitrogen atmosphere prior to use. Deuterated solvents were dried over sodium, degassed and distilled in a nitrogen atmosphere. The yields given are not optimized. ^1H, $^{13}C\{^1H\}$, and ^{31}P NMR spectra were recorded on Bruker Avance III 400 MHz (BBO or BBFO) and Bruker Avance IV (NEO) 500 MHz (Prodigy BBO or Diff50 (DOSY)) spectrometers. Chemical shifts are reported in parts per million relative to $SiMe_4$, LiCl and aqueous phosphoric acid as external standards. The residual signals of the deuterated solvents $[D_8]$THF, $[D_8]$toluene and $[D_6]$benzene were used as internal standards for the interpretation of ^1H NMR spectra. The ^1H, $^{13}C\{^1H\}$, and ^{31}P NMR spectra are depicted in the Supporting Information. Substrates were purchased from abcr, Alfa Aesar, Merck or TCI and used without further purification. The Schiff bases **1a** and **1b** were prepared in a similar procedure as described earlier.[21] The carbon values of the Ti and Zr complexes **2a** and **3** are low due to carbide and carbonate formation during combustion.

Synthesis of 2,2′-bis[2-hydroxy-3,5-di(*tert*-butyl)benzylideneamino]-1,1′-biphenyl (**1a**): The *Schiff* base **1a** was synthesized via condensation reaction of 3,5-di(*tert*- butyl)salicylaldehyde with 2,2′-diamino-1,1′-biphenyl. In a 100 ml round bottom flask 3,5-di(*tert*-butyl)salicylaldehyde (5.44 g, 23.2 mmol) was dissolved in 55 ml of anhydrous methanol. To the stirred solution of 3,5-di(*tert*-butyl)salicylaldehyde, 15 ml of a methanolic solution of 2,2′-diamino-1,1′-biphenyl (2.14 g, 11 mmol) were added and this mixture refluxed for 3 h. During cooling to room temperature, a yellow solid started to precipitate. Cooling of the solution to +5 °C gave **1a** as a yellow powder. Filtration through celite and washing of the solid with anhydrous methanol (10 ml) yielded pure **1a** (5.80 g, 81 %). Single crystals of **1a** grew by storing the reaction solution after filtration overnight at room temperature. ^1H NMR ($[D_8]$THF): δ = 13.07 (s, 2H, OH), 8.64 (s, 2H, N=CH), 7.09 (d, 2H, phenolic ArH),7.29 (d, 2H, phenolic ArH), 7.31–7.45 (m, 8H, biaryl H), 1.34 (s, 18H, *t*Bu), 1.23 (s, 18H, *t*Bu). $^{13}C\{^1H\}$ NMR ($[D_8]$THF): δ = 164.2 (N=C), 157.9 (CO), 147.5 (biaryl-N=C), 139.6 (C*t*Bu), 135.8 (C*t*Bu), 135.1, 130.5, 128.6, 127, 126.9, 126.2, 118.7, 117.8, 34.6 (CMe), 33.7 (CMe), 30.8 (Me), 28.8 (Me). Elemental analysis ($C_{42}H_{52}N_2O_2$, 616.89): calcd.: C 81.78, H 8.50, N 4.54; found: C 81.47, H 8.40, N 4.62. MS (EI, m/z) (%): 616 (50) $[M^+]$, 601 (5) $[M^+-CH_3]$, 559 (10) $[M^+-Bu^t]$, 384 (25), 293(45), 180 (100), 57 (55). IR (ATR, cm^{-1}): 2945 (m), 2904 (m), 2870 (m), 1617 (s), 1587 (m), 1560 (m), 1480 (m), 1460 (m), 1440 (s), 1389 (m), 1360 (m), 1248 (m), 1195 (m), 1170 (s), 1132 (w), 1099 (w), 1022 (w), 966 (w), 873 (s), 826 (s), 799 (m), 756 (s), 746 (s), 732 (m), 640 (m), 609 (w), 522 (m). M.p. = 126.2–127.0 °C.

Synthesis of 2,2′-bis[2-hydroxy-3,5-di(*tert*-butyl)benzylideneamino]-4,4′-dimethyl-1,1′-biphenyl (**1b**): A mixture of 0.65 mmol of 2,2′-diamino-4,4′-dimethyl-1,1′-biphenyl and 1.30 mmol of 3,5-di(tert-butyl)salicylaldehyde in ethanol (12 ml) was stirred and refluxed for 4 h. During the reaction, the corresponding *Schiff* base **1b** precipitated as a colored solid. The solid was collected by filtration, washed with cold ethanol and dried in vacuo. Yield 0.27 g, 64 %. Elemental analysis ($C_{44}H_{56}N_2O_2$, 644.94): calcd.: C 81.94, H 8.75, N 4.34; found: C 81.87, H 8.74, N 4.32. MS (EI, m/z): 645 $[M]^+$. IR (ATR, cm^{-1}): 3032 (w, OH), 2857 (s, *t*Bu), 1609 (s, C=N), 1483 (s); 1391 (s). ^1H NMR ($CDCl_3$): δ = 13.08 (s, 2H, OH), 8.49 (s, 2H, N=CH), 7.00–7.28 (m, 10H, phenolic and biaryl H), 2.43 (s, 6H, Me), 1.35 (s, 18H, *t*Bu), 1.23 (s, 18H, *t*Bu). $^{13}C\{^1H\}$ NMR ($CDCl_3$): δ = 163.4 (N=C), 158.1 (CO), 147.5 (biaryl-N=C), 139.9 (C*t*Bu), 138.7, 136.5 (C*t*Bu), 132.1, 130.7, 127.4, 127.3, 126.8, 118.7, 118.5, 35.1 (CMe), 34.2 (CMe), 31.6 (Me), 29.4 (Me), 21.4 (Me).

Synthesis of Ti complex **2a**: *Schiff* base **1a** was converted to its disodium salt with sodium hydride in THF. A solution of **1a** (1 g, 1.621 mmol) in anhydrous THF (15 ml) was added dropwise to the suspension of NaH (0.0778 g, 3.241 mmol) in THF (15 ml). Hydrogen gas was released. The mixture was stirred at room temperature for 24 h. During this time, almost the entire NaH was consumed. The progress of the reaction was monitored by ^1H NMR spectroscopy. The mixture was filtered to remove excess of NaH. A solution of $[(thf)_2TiCl_4]$ (0.541 g, 1.62 mmol) in THF (15 ml) was added dropwise to the previous solution. Immediately thereafter, the color of the reaction solution changed from yellow to red. The mixture was stirred at room temperature for 24 h and then THF removed under reduced pressure. Red crystals of the Ti complex **2a** (0.77 g, 64.75 %) crystallized from mixtures of toluene/hexane or diethyl ether/pentane. Integration of signals in the ^1H NMR spectrum indicated the formation of the *trans* and *cis*-β isomers with a ratio of 1 : 2.84. ^1H NMR (C_6D_6): δ = 7.82 (s, 0.70H, *trans* N=CH), 7.70 (s, 1H, *cis*-β N=CH), 7.60 (s, 1H, *cis*-β N=CH), 6.26–7.77 (m, *trans* and *cis*-β phenolic and biaryl H), 1.75 (s, 9H, *cis*-β *t*Bu), 1.75 (s, 6.33H, *trans* *t*Bu), 1.68 (s, 9H, *cis*-β *t*Bu), 1.22 (s, 6.33H, *trans* *t*Bu), 1.20 (s, 9H, *cis*-β *t*Bu), 1.06 (s, 9H, *cis*-β *t*Bu). $^{13}C\{^1H\}$ NMR (C_6D_6): δ = 170.1 (*trans* N=C), 168.9 (*cis*-β N=C), 168.0 (*cis*-β N=C), 162.2, 161.3, 152.1, 151.8, 151.1, 143.8 (*trans* C*t*Bu), 143.4 (*cis*-β C*t*Bu), 143.1 (*cis*-β C*t*Bu), 136.4 (*trans* C*t*Bu), 136.3 (*cis*-β C*t*Bu), 136.2 (*cis*-β C*t*Bu), 132.9, 132.5, 132.3, 131.3, 131.2, 130.8, 129.7, 129, 128.9, 128.7, 128.5, 128.2, 127.1, 126.1, 125.3, 125.1, 124.7, 123.7, 35.7 (*trans* CMe), 35.3 (*cis*-β CMe), 35.2 (*cis*-β CMe), 34.2 (*trans* CMe), 34.1 (*cis*-β CMe), 33.9 (*cis*-β CMe), 31.1 (*cis*-β and *trans* Me), 30.8 (*cis*-β Me), 30.0 (*trans* Me), 29.9 (*cis*-β Me), 29.8 (*cis*-β Me). Elemental analysis ($C_{42}H_{50}Cl_2N_2O_2Ti$, 733.64): calcd.: C 68.76, H 6.87, N 3.82; found: C 66.61, H 6.87, N 3.75. MS (EI, m/z) (%): 700 (20) $[M^+-2Me-3H]$, 697 (100) $[M^+-Cl]$, 662 (< 5) $[M^+-2Cl]$, 625 (< 5), 207 (10). IR (ATR, cm^{-1}): 2954 (m), 1601 (m), 1586 (m), 1556 (s), 1543 (s), 1497 (w), 1476 (m), 1463 (m), 1433 (m), 1409 (m), 1392 (m), 1377 (m), 1360 (m), 1271 (s), 1249 (s), 1202 (m), 1178 (s), 1133 (m), 1096 (m), 1029 (m), 975 (m), 919 (m), 863 (m), 846 (s), 813 (m), 766 (s), 753 (m), 740 (s), 695 (m).

Synthesis of Ti complex **2b**: The sodium salt of **1b** was prepared *in situ* via the addition of 0.02 g of solid NaH (0.83 mmol) to a solution of 0.25 g of *Schiff* base **1b** (0.39 mmol) in 10 ml of THF. A slightly yellow suspension formed which was stirred for 24 h. Then, 0.13 g of $[(thf)_2TiCl_4]$ (0.39 mmol) were added and the reaction mixture stirred for additional 12 h. The solvent was removed in vacuo and the residue extracted with acetonitrile. The volume of this red solution was reduced and 0.18 g of red crystals of Ti complex **2b** (61 %) precipitated at r.t. Elemental analysis ($C_{44}H_{54}Cl_2N_2O_2Ti$, 761.70): calcd.: C 69.38, H 7.15, N 3.68; found: C 69.36, H 7.12, N 3.62. MS (EI, m/z): 762 $[M]^+$. IR (ATR, cm^{-1}): 2852 (s);

1615 (s); 1485 (s); 1356 (s); 598 (m); ν 468 (w). The ^{1}H (Figure S7) and ^{13}C{^{1}H} NMR (Figure S8) spectra are depicted in the Supporting Information, a reliable assignment of the resonances is impossible.

Synthesis of Zr complex **3**: Compound **3** was synthesized in an analogous manner to compound **2**. Firstly, the disodium salt of **1 a** was prepared following the general method as described for compound **2** from **1 a** (1.06 g, 1.72 mmol) and NaH (0.097 g, 4.04 mmol). Then [(thf)$_2$ZrCl$_4$] (0.655 g, 1.74 mmol), dissolved in anhydrous THF (15 ml), was added to the disodium salt solution of the Schiff base. The mixture was stirred at room temperature for 24 h and then, THF removed under reduced pressure. Yellow crystals of the Zr complex **3** (1.01 g, 76 %) precipitated and were recrystallized from a THF/pentane mixture. ^{1}H NMR (C_6D_6): δ = 7.65 (s, 2H, N=CH), 6.72–7.69 (m, 12H, phenolic and biaryl H), 1.71 (s, 18H, *t*Bu), 1.13 (s, 18H, *t*Bu). ^{13}C{^{1}H} NMR (C_6D_6): δ = 171.8 (*cis*-α N=C), 159.1 (*cis*-α biaryl-N=C), 150.5 (*cis*-α CO), 141.7 (*cis*-α C*t*Bu), 138.6 (*cis*-α C*t*Bu), 133.0, 132.3 (*cis*-α phenolic C), 129.9, 129.3 (*cis*-α phenolic C), 129.1, 124.8, 123.2 (*cis*-α phenol-N=C), 35.3 (*cis*-α CMe), 33.9 (*cis*-α CMe), 30.9 (*cis*-α Me), 29.6 (*cis*-α Me). Elemental analysis ($C_{42}H_{50}Cl_2N_2O_2Zr$, 777.12): calcd.: C 64.92, H 6.49, N 3.61; found: C 62.18, H 6.33, N 3.60. MS (EI, m/z): 777 (52) [M^+], 723 (40), 650 (45), 373 (42), 355 (100), 336 (22), 167 (20). IR (ATR, cm^{-1}): 2954 (m), 2864 (m), 1605 (m), 1584 (s), 1556 (m), 1541 (s), 1463 (s), 1442 (s), 1431 (s), 1407 (m), 1383 (s), 1360 (s), 1297 (m), 1273 (s), 1252 (s), 1200 (m), 1176 (s), 1133 (m), 1094 (m), 1042 (m), 1031 (m), 997 (m), 982 (m), 962 (m), 947 (m), 932 (m), 911 (m), 887 (w), 878 (m), 865 (m), 855 (s), 842 (s), 813 (m), 777 (m), 768 (s), 749 (s), 708 (m), 701 (m).

Preparation of complex **4**: Ti(NMe$_2$)$_4$ (0.15 ml, 0.633 mmol, d = 0.947 g/ml) was added dropwise at room temperature to a solution of **1 a** (0,381 g, 0.617 mmol) in anhydrous *n*-pentane (5 ml). Immediately the color of the reaction solution changed from yellow to red and the mixture was stirred for 5 h. Removal of both acidic phenolic protons led to liberation of 2 mol of dimethylamine. Reduction of the volume of the solution under reduced pressure led to precipitation of red crystals of **4**. However, pure compound 4 could not be isolated because an oily residue remained and covered the crystalline material. ^{1}H NMR from the reaction solution (C_6D_6): δ = 6.79–7.62 (m, 12H, ArH), 5.24 (s, 2H, N–CH), 2.67 (s, 6H, NMe$_2$), 2.12 (s, 6H, NMe$_2$), 1.45 (s, 36H, *t*Bu); resonances of lower intensity arise from other isomers (see Supporting Information). MS (EI, m/z): 750 (< 1) [M^+], 775 (31), 708 (54), 707 (100), 706 (15) [M^+ − NMe$_2$], 679 (13).

Crystal structure determinations: The intensity data for the compounds were collected on a Nonius KappaCCD diffractometer using graphite-monochromated Mo-K$_\alpha$ radiation. Data were corrected for Lorentz and polarization effects; absorption was taken into account on a semi-empirical basis using multiple-scans.[22–25] The structures were solved by intrinsic methods (SHELXT)[26] and refined by full-matrix least squares techniques against F_o^2 SHELXL-2018[27]). The hydrogen atoms bonded to the hydroxy- group O1 of **1 a**, to the chiral carbon atoms C7 and C20 of **4**, and all hydrogen atoms of **1 b** (except those bonded at C11) were located by difference Fourier synthesis and refined isotropically. All other hydrogen atoms were included at calculated positions with fixed thermal parameters. The crystal of **2 b** contains large voids, filled with disordered solvent molecules. The size of the voids is 869 Å^3/unit cell. Their contribution to the structure factors was secured by back-Fourier transformation using the SQUEEZE routine of the program PLATON[28] resulting in 301 electrons/unit cell). All non-hydrogen atoms were refined anisotropically.[27] Crystallographic data as well as structure solution and refinement details are summarized in Table S1. XP[29] and POV-Ray[30] were used for structure representations.

Supporting Information (see footnote on the first page of this article): NMR spectra, crystallographic and refinement details of crystal structures, molecule representations of **1 a** and **2 b** as well as computational details (pdf file).

Deposition Numbers 2176797 (for 1a), 2176798 (for 1b), 2176799(for 2a), 2176800 (for 2b), 2176801 (for **3**), and 2176802 (for 4) contain the supplementary crystallographic data for this paper. These data are provided free of charge by the joint Cambridge Crystallographic Data Centre and Fachinformationszentrum Karlsruhe Access Structures service www.ccdc.cam.ac.uk/structures.

Acknowledgements

*We acknowledge the valuable support of the NMR service platform (www.nmr.uni-jena.de) and of the mass spectrometry platform (www.ms.uni-jena.de) of the Faculty of Chemistry and Earth Sciences of the Friedrich Schiller University Jena, Germany. We thank Dr. Philipp Schüler for providing VT-NMR and EXSY spectra of compound **2 a**. B. R. K. thanks the German Academic Exchange Service (DAAD, grant no. 57440921) for a generous Ph.D. grant. T. M. A. A. and M. W. are grateful to the German Research Foundation (DFG, project no. We 1561/21-3) for financial support. Open Access funding enabled and organized by Projekt DEAL.*

Conflict of Interest

The authors declare no conflict of interest.

Data Availability Statement

The data that support the findings of this study are available in the supplementary material of this article.

Keywords: Bailar twist · ONNO ligands · Schiff bases · Titanium · Zirconium

[1] a) T. Katsuki, *Coord. Chem. Rev.* **1995**, *140*, 189–214; b) L. Canali, D. C. Sherrington, *Chem. Soc. Rev.* **1999**, *28*, 85–93; c) T. P. Yoon, E. N. Jacobsen, *Science* **2003**, *299* (5613), 1691–1693; d) T. Katsuki, *Synlett* **2003**, 281–297; e) P. G. Cozzi, *Chem. Soc. Rev.* **2004**, *33*, 410–421; f) T. Katsuki, *Chem. Soc. Rev.* **2004**, *33*, 437–444; g) T. R. J. Achard, L. A. Clutterbuck, M. North, *Synlett* **2005**, 1828–1847; h) N. S. Venkataramanan, G. Kuppuraj, S. Rajagopal, *Coord. Chem. Rev.* **2005**, *249*, 1249–1268; i) C. Baleizao, H. Garcia, *Chem. Rev.* **2006**, *106*, 3987–4043; j) K. Matsumoto, B. Saito, T. Katsuki, *Chem. Commun.* **2007**, 3619–3627; k) S. J. Wezenberg, A. W. Kleij, *Angew. Chem. Int. Ed.* **2008**, *47*, 2354–2364; *Angew. Chem.* **2008**, *120*, 2388–2399; l) K. C. Gupta, A. K. Sutar, *Coord. Chem. Rev.* **2008**, *252*, 1420–1450; m) A. W. Kleij, *Chem. Eur. J.* **2008**, *14*, 10520–10529; n) A. W. Kleij, *Eur. J. Inorg. Chem.* **2009**, 193–205; o) A. W. Kleij, *Dalton Trans.* **2009**, 4635–4639; p) S. Akine, T. Nabeshima, *Dalton Trans.* **2009**, 10395–10408; q) A. D. Cort, P. De Bernardin, G. Forte, F. Y. Mihan, *Chem. Soc. Rev.* **2010**, *39*, 3863–3874; r) A. Decortes, A. M. Castilla, A. W. Kleij, *Angew. Chem. Int. Ed.* **2010**, *49*, 9822–9837; *Angew. Chem.* **2010**, *122*, 10016–10032; s) T. Glaser, *Chem. Commun.* **2011**, *47*, 116–130; t) C. J. Whiteoak, G. Salassa, A. W. Kleij, *Chem. Soc. Rev.* **2012**, *41*, 622–631; u) C. P. Pradeep, S. K. Das, *Coord. Chem. Rev.*

2013, *257*, 1699–1715; v) R. M. Clarke, T. Storr, *Dalton Trans.* **2014**, *43*, 9380–9391; w) R. M. Clarke, K. Herasymchuk, T. Storr, *Coord. Chem. Rev.* **2017**, *352*, 67–82; x) H.-Y. Yin, J. Tang, J.-L. Zhang, *Eur. J. Inorg. Chem.* **2017**, 5085–5093; y) I. M. Marín, A. Auffrant, *Eur. J. Inorg. Chem.* **2018**, 1634–1644; z) A. Erxleben, *Inorg. Chim. Acta* **2018**, *472*, 40–57; aa) M. A. El Sater, N. Jaber, E. Schulz, *ChemCatChem* **2019**, *11*, 3662–3587; ab) J. C. Pessoa, I. Correia, *Coord. Chem. Rev.* **2019**, *388*, 227–247; ac) M. Karmakar, S. Chattopadhyay, *J. Mol. Struct.* **2019**, *1186*, 155–186; ad) S. Shaw, J. D. White, *Chem. Rev.* **2019**, *119*, 9381–9426; ae) A. Lidskog, Y. Li, K. Wärnmark, *Catalysts* **2020**, *10*, 705; af) S. M. Elbert, M. Mastalerz, *Org. Mat.* **2020**, *2*, 182–203; ag) J. Min, Z. Xia, T. Zhang, H. Su, Y. Zhi, S. Shan, *Chem. Pap.* **2021**, *75*, 2965–2980; ah) Y.-C. Yuan, M. Mellah, E. Schulz, O. R. P. David, *Chem. Rev.* **2022**, *122*, 8841–8883.

[2] T. M. A. Al-Shboul, S. Ziemann, H. Görls, T. M. A. Jazzazi, S. Krieck, M. Westerhausen, *Eur. J. Inorg. Chem.* **2018**, 1563–1570.

[3] S. J. Coles, M. B. Hursthouse, D. G. Kelly, A. J. Toner, N. M. Walker, *J. Chem. Soc. Dalton Trans.* **1998**, 3489–3494.

[4] G. Gilli, D. W. J. Cruickshank, R. L. Beddoes, O. S. Mills, *Acta Crystallogr. Sect. B* **1972**, *28*, 1889–1893.

[5] E. Solari, C. Floriani, A. Chiesi-Villa, C. Rizzoli, *J. Chem. Soc. Dalton Trans.* **1992**, 367–373.

[6] H. Chen, P. S. White, M. R. Gagné, *Organometallics* **1998**, *17*, 5358–5366.

[7] P. R. Woodman, N. W. Alcock, I. J. Munslow, C. J. Sanders, P. Scott, *J. Chem. Soc. Dalton Trans.* **2000**, 3340–3346.

[8] L. Chen, N. Zhao, Q. Wang, G. Hou, H. Song, G. Zi, *Inorg. Chim. Acta* **2013**, *402*, 140–155.

[9] P. Woodman, P. B. Hitchcock, P. Scott, *Chem. Commun.* **1996**, 2735–2736.

[10] P. R. Woodman, I. J. Munslow, P. B. Hitchcock, P. Scott, *J. Chem. Soc. Dalton Trans.* **1999**, 4069–4076.

[11] P. D. Knight, G. Clarkson, M. L. Hammond, B. S. Kimberley, P. Scott, *J. Organomet. Chem.* **2005**, *690*, 5125–5144.

[12] P. D. Knight, P. N. O'Shaughnessy, I. J. Munslow, B. S. Kimberley, P. Scott, *J. Organomet. Chem.* **2003**, *683*, 103–113.

[13] M. Zauliczny, R. Grubba, L. Ponikiewski, J. Pikies, *Polyhedron* **2017**, *123*, 353–360.

[14] D. Andrae, U. Häußermann, M. Dolg, H. Stoll, H. Preuß, *Theor. Chim. Acta* **1990**, *77*, 123–141.

[15] A. Bergner, M. Dolg, W. Küchle, H. Stoll, H. Preuß, *Mol. Phys.* **1993**, *80*, 1431–1441.

[16] Y. Zhao, D. G. Truhlar, *J. Phys. Chem. A* **2005**, *109*, 5656–5667.

[17] J. Kreutzer, P. Blaha, U. Schubert, *Comput. Theor. Chem.* **2016**, *1084*, 162–168.

[18] Y. Zhao, D. G. Truhlar, *Theor. Chem. Acc.* **2008**, *120*, 215–241.

[19] S. Grimme, J. Antony, S. Ehrlich, H. Krieg, *Chem. Phys.* **2010**, *132*, 154104.

[20] M. J. Frisch, G. W. Trucks, H. B. Schlegel, G. E. Scuseria, M. A. Robb, J. R. Cheeseman, G. Scalmani, V. Barone, G. A. Petersson, H. Nakatsuji, X. Li, M. Caricato, A. V. Marenich, J. Bloino, B. G. Janesko, R. Gomperts, B. Mennucci, H. P. Hratchian, J. V. Ortiz, A. F. Izmaylov, J. L. Sonnenberg, D. Williams-Young, F. Ding, F. Lipparini, F. Egidi, J. Goings, B. Peng, A. Petrone, T. Henderson, D. Ranasinghe, V. G. Zakrzewski, J. Gao, N. Rega, G. Zheng, W. Liang, M. Hada, M. Ehara, K. Toyota, R. Fukuda, J. Hasegawa, M. Ishida, T. Nakajima, Y. Honda, O. Kitao, H. Nakai, T. Vreven, K. Throssell, J. A. Montgomery, Jr., J. E. Peralta, F. Ogliaro, M. J. Bearpark, J. J. Heyd, E. N. Brothers, K. N. Kudin, V. N. Staroverov, T. A. Keith, R. Kobayashi, J. Normand, K. Raghavachari, A. P. Rendell, J. C. Burant, S. S. Iyengar, J. Tomasi, M. Cossi, J. M. Millam, M. Klene, C. Adamo, R. Cammi, J. W. Ochterski, R. L. Martin, K. Morokuma, O. Farkas, J. B. Foresman, D. J. Fox, Gaussian 16 Rev. B.01, Gaussian, Inc., Wallingford CT, **2016**.

[21] a) L. Clowes, M. Walton, C. Redshaw, Y. Chao, A. Walton, P. Elo, V. Sumerin, D. L. Hughes, *Catal. Sci. Technol.* **2013**, *3*, 152–160; b) R. Kunert, C. Philouze, F. Berthiol, O. Jarjayes, T. Storr, F. Thomas, *Dalton Trans.* **2020**, *49*, 12990–13002.

[22] R. Hooft: COLLECT, Data Collection Software; Nonius B. V., Netherlands, **1998**.

[23] Z. Otwinowski, W. Minor, in *Methods in Enzymology* (Eds. C. W. Carter, R. M. Sweet), vol. *276*, part A, Academic Press, San Diego, USA, **1997**, pp. 307–326.

[24] a) SADABS 2.10, Bruker-AXS Inc., **2002**, Madison, WI, USA; b) SADABS 2016/2: L. Krause, R. Herbst-Irmer, G. M. Sheldrick, D. Stalke, *J. Appl. Crystallogr.* **2015**, *48*, 3–10.

[25] Bruker (**2020**) APEX3 Bruker AXS LLC, Madison, WI, USA.

[26] G. M. Sheldrick, *Acta Crystallogr. Sect. A* **2015**, *71*, 3–8.

[27] G. M. Sheldrick, *Acta Crystallogr. Sect. C* **2015**, *71*, 3–8.

[28] A. L. Spek, *Acta Crystallogr. Sect. C* **2015**, *71*, 9–18.

[29] XP, Siemens Analytical X-ray Instruments Inc., Karlsruhe, Germany, **1990**; Madison, WI, USA, **1994**.

[30] POV-Ray, Persistence of Vision Raytracer, Victoria, Australia, **2007**.

Manuscript received: August 17, 2022
Revised manuscript received: September 29, 2022
Accepted manuscript online: October 10, 2022